

Mixing natural and synthetic surfactants: co-adsorption of triterpenoid saponins and sodium dodecyl sulfate at the air-water interface.

I M Tucker¹, A Burley¹, R. E. Petkova¹, S. L. Hosking¹, J Penfold^{2,3#}, R K Thomas³, P X Li², J R P Webster², R Welbourn²

1. Unilever Research and Development, Port Sunlight Laboratory, Quarry Road East, Bebington, Wirral, UK
2. ISIS Facility, STFC, Rutherford Appleton Laboratory, Chilton, Didcot, OXON, UK
3. Physical and Theoretical Chemistry Laboratory, Oxford University, South Parks Road, Oxford, UK

Corresponding Author: Professor Jeff Penfold, phone: +44 1235 445681, email: jeff.penfold@stfc.ac.uk

Keywords: Mixed surfactant adsorption, saponins, escin, sodium dodecyl sulfate, neutron reflectivity, air-water interface, pseudo phase approximation.

ABSTRACT

Saponins are highly surface active glycosides, derived from a wide range of plant species. Their ability to produce stable foams and emulsions has stimulated their applications in beverages, foods, and cosmetics. To explore a wider range of potential applications their surface mixing properties with conventional surfactants have been investigated. The competitive adsorption of the triterpenoid saponin escin with the anionic surfactant sodium dodecyl sulfate, SDS, at the air-water interface has been studied by neutron reflectivity, NR, and surface tension, ST. The NR measurements, at concentrations above the mixed critical micelle concentration, cmc, demonstrate the impact of the relative surface activities of the two components. The surface mixing is highly non-ideal, and can be described quantitatively by the pseudo phase approximation with the inclusion of the quadratic and cubic terms in the excess free energy of mixing. Hence the surface mixing is highly asymmetrical and reflects both the electrostatic and steric contributions to the inter-molecular interactions. The relative importance of the steric contribution is reinforced by the observation that the micelle mixing is even more non-ideal than the surface mixing. The mixing properties result in the surface adsorption being largely dominated by the SDS over the composition and concentration range explored. The results and their interpretation provide an important insight into the wider potential for mixing saponins with more conventional surfactants.

INTRODUCTION

The saponins are highly surface active glycosides, which are present in a wide range of plant species (1-5). The surface activity of the saponins results from the presence of a hydrophobic scaffold which comprises of a triterpenoid, steroid or steroid-alkaloid group, and a hydrophilic part which consists of different saccharide residues which are linked to the hydrophobic scaffold via glycoside bonds. There is a wide range of molecular structures found within the different plant species and often within the same plant species (3). This wide range of molecular structures gives rise to a wide range of physicochemical properties, biological activity and function. The intrinsic surface activity of the saponins is the basis of their use as foam stabilisers in beverages such as beer and soft drinks (1, 4, 6), in emulsion stabilisation (1, 6), and solubilisation of additives (7) in foods. Different aspects of their biological activity are the basis of their use as natural medicines (8, 9). However saponins exhibit anti-inflammatory, anti-fungal, anti-bacterial, anti-viral, anti-cancer properties, and cholesterol lowering potential. These properties make them increasingly important in applications in cosmetics, shampoos and conditioners, and in skin anti-ageing products (10, 11).

The surface activity and the wide range of complementary properties of saponins make them potentially important for an even wider range of applications (4). In light of this the adsorption properties of saponins has been extensively studied (12-21), and their self-assembly in solution characterised (22-30). Furthermore their mixing properties with a range of proteins has been studied (30-35). However, in terms of extending the range of applications of saponins, their mixing behaviour with a range of conventional synthetic surfactants is likely to be key factor, and this has been studied much less extensively (36-38). The focus of this paper is to address that issue and study the co-adsorption of saponins with the anionic surfactant SDS.

The surface adsorption of a range of different saponins, including the escin, tea and Quillaja saponins, has recently been studied by NR, ST (39) and molecular dynamics simulations (40). Their high surface activity gives rise to relatively low cmc values, ($\sim 100\mu\text{M}$), comparable to many nonionic surfactants. The saturation adsorption is largely independent of pH, consistent with the assumption that they behave like nonionic surfactants. However the cmc can depend upon pH, and for escin decreases significantly with decreasing pH. The ability of saponins to stabilise foams and emulsions so effectively arises from a different and unusual surface property. The surface adsorbed layers formed are highly rigid, exhibiting high surface moduli and shear visco-elasticity (12-17). The high surface elasticity is indicative of a densely packed

solid-like surface layer. This implies strong inter-molecular interactions, which are assumed to arise from multiple hydrogen bonds between neighbouring sugar groups. The recent NR measurements on escin and tea saponin adsorbed layers (39) show that the structure of the adsorbed layer is dominated by a relatively dense and hydrated headgroup region. In contrast the hydrophobic triterpenoid region is less densely packed and contains no solvent. These structural features support the supposition that the origin of the high surface viscoelasticity is due to inter-molecular hydrogen bonding. This has been further reinforced by recent molecular dynamics simulations (40).

The competitive adsorption at the interface of Quillaja bark saponin in conjunction with lysozyme, β -casein, and β -lactoglobulin has been recently reported (31-35). In general the surface behaviour is similar to that observed in protein / synthetic surfactant mixtures. That is, the Saponin displaces the protein at the interface at high surfactant concentrations. However, specific interactions between the saponin and proteins results in a more complex behaviour (33). This can also have a profound effect on the surface rheology. There have, however, been very few detailed studies on the adsorption of saponins with different synthetic surfactants. Jian et al (37) have studied the mixing of tea saponin, TS, with SDS, cetyltrimethyl ammonium bromide, CTAB, and the nonionic surfactant Brij35 by ST and foam stability measurements. They report a synergistic ST and cmc lowering and enhanced foam stability for the TS / SDS and TS / CTAB mixtures, but not for the TS / Brij35 mixture. This was largely attributed to the TS acting as a nonionic component in the mixture, reducing headgroup interactions to produce highly non-ideal mixing.

The focus of this paper is the study of the adsorption of the triterpenoid saponin escin with the anionic surfactant SDS at the air-water interface. The adsorption is characterised using NR and ST. In recent years it has been demonstrated that NR is an important probe of surfactant (41) and mixed surfactant (41-43) adsorption; and adsorbed amounts, surface compositions and structural information can be determined directly. The concentration / composition range explored was chosen to obtain maximum sensitivity to the effects of the departure from ideal mixing (42, 43), and to address concentration ranges relevant to potential applications; and so are mainly at concentrations in excess of the critical micelle concentration, cmc.

EXPERIMENTAL DETAILS

(i) Surface Tension

Surface tension measurements were carried out using an automated Kruss K100T force tensiometer with double Dosino titration system, fitted with a standard Wilhelmy plate. The plate was cleaned with Decon90, water, ethanol, and water sequentially and finally flamed under butane corona before measurements were made. The calibration was checked by measuring the surface tension of UHQ water, (72.2 mN/m). A series of dilutions were used to generate the surface tension versus concentration data for a variety of mixtures. The solutions were first prepared at the highest concentration above the cmc at the desired composition. The solutions were prepared in UHQ water containing 0.1M NaCl, buffered to pH8 using NaOH. The solutions were warmed gently to achieve full dissolution with gentle stirring. The tensiometer was programmed to wait at each dilution until the surface tension was reproduced to an accuracy of ± 0.1 mN/m before proceeding to the next dilution. This was generally no more than 2400 seconds at maximum dilution. All the measurements were made at a temperature of $25 \pm 0.5^\circ\text{C}$.

(ii) Neutron Reflectivity

Neutron reflectivity is now an established method for studying surfactant and mixed surfactant adsorption at interfaces, providing an absolute determination of adsorbed amounts, and structural details of the adsorbed layer (41). In the kinematic approximation (41) the neutron reflectivity $R(Q)$ (Q is the wave vector transfer perpendicular to the surface, $Q=4\pi\sin\theta/\lambda$, θ is the grazing angle of incidence, and λ the neutron wavelength) from a planar surface is directly related to square of the Fourier transform of the scattering length density, $\rho(z)$ ($\rho(z)$ is defined as $\rho(z)=\sum_i b_i n_i(z)$, where $n_i(z)$ is the number density of species i and b_i its neutron scattering length). $\rho(z)$ can be manipulated using D/H isotopic substitution, as the neutron scattering lengths of H and D are -3.75×10^{-5} and 6.67×10^{-5} Å. A 92 mole % H_2O / 8 mole % D_2O mixture, null reflecting water, nrw, has a scattering length density of zero, and hence a refractive index the same as air. For a monolayer of deuterium labelled surfactant adsorbed at such an air-water interface the reflectivity arises only from the adsorbed layer. In that case the reflectivity can be expressed exactly as (41),

$$R = \frac{16\pi^2}{Q^4} (2\rho)^2 \sin^2\left(\frac{Qd}{2}\right) \quad (1)$$

where d and ρ are the thickness and scattering length density of the adsorbed layer. For a single surfactant species at the interface the area/molecule is related to the product $d \cdot \rho$ and the $\sum b$ value (see table 1) of the surfactant, such that (41),

$$A = \frac{\sum b}{d\rho} \quad (2)$$

and the surface excess, Γ , is given by $\Gamma=1/N_a A$. For the binary mixtures reported here equation 2 becomes,

$$d\rho = \frac{\sum b_1}{A_1} + \frac{\sum b_2}{A_2} \quad (3)$$

Table 1. $\sum b$ values for the different surfactant components

Component	$\sum b$ ($\times 10^{-3}$ Å)
d-SDS	2.763
h-SDS	0.152
escin	1.78

For the mixtures of the saponins with SDS, deuterium labelled saponins are not available, but the $\sum b$ for the saponins without deuterium labelling provides a sufficient contrast against nrw (39). Here two reflectivity measurements were made in nrw for the isotopic combinations, d-SDS / saponin and h-SDS / saponin. The resulting simultaneous equations (equation 3) can be solved to determine the adsorbed amount of each component in the binary mixture. This approach has now been applied to a range of binary and multi-component mixtures (41-43).

The NR measurements were made on the INTER (44) and SURF (45) reflectometers at the ISIS pulsed neutron source. In both cases the reflectivity, $R(Q)$, was measured over a broad range of Q , at a fixed angle of incidence, θ , and a wide range of neutron wavelengths, λ , sorted by time of flight. On INTER the measurements were made at two angle of incidence, 0.8 and 2.3 °, and a λ range of 0.5 to 15 Å, to cover a Q range of 0.01 to 0.5 Å⁻¹. On SURF a fixed angle of incidence of 1.5° and a λ range of 0.5 to 6.8 Å were used to cover a Q range of 0.048 to 0.5 Å⁻¹. The reflected intensity was normalised to the direct beam and set to an absolute reflectivity scale by reference to the reflectivity from a D₂O surface. The samples were contained in sealed Teflon troughs, containing sample volumes ~ 25 mL, and held at 25°C. Each individual measurement took ~ 30 to 60 minutes, and the measurements were made in sequence in a 5 or 7 position sample changer. Repeated measurements gave no indication of any time dependence in the adsorption.

(iii) Materials

The escin used in this study was obtained from Sigma Aldrich (part no E1378, batch no BLCV8469V_3). It was 96% pure and was used as received. The structure of escin is shown in figure 1.

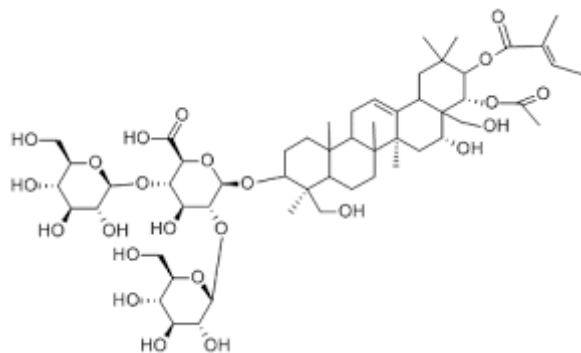


Figure 1. Structure of escin

The d-SDS was synthesised at the ISIS Isotope Facility using well established synthetic routes. It was recrystallized from ethanol, and its purity verified by NR and ST measurements (44). The h-SDS was purchased from Sigma Aldrich and was recrystallized three times from hot ethanol, according to established procedures at Unilever R&D Port Sunlight. All the measurements were made in 0.1 M NaCl. The NaCl and D₂O (99.9%) were obtained from SIGMA, and high purity water (Elga Ultrapure) was used throughout. All the glassware and Teflon troughs used were cleaned in dilute Decon90 solutions and rinsed in high purity water.

(iv) Measurements made

Three different sequences of NR measurements were made. Measurements were made for SDS / escin mixtures at fixed concentrations of 0.3 and 1.5 mM, and variable SDS / escin solution compositions from 0/100 to 100/0 mole ratio. Measurements were made at a 50/50 mole ratio SDS / escin mixture and variable solution concentrations from 0.1 to 1.5 mM. At a fixed escin concentration of 0.01 wt% (9×10^{-5} M) measurements were made for the SDS / escin mixture

with variable SDS concentrations from 0.1 to 5 mM. All the measurements were made in 0.1 M NaCl and in nrw. For the binary mixtures two different ‘contrasts’ were measured, for the combinations d-SDS / saponin, and h-SDS / saponin.

(v) Thermodynamics of mixing

The departures from ideality are quantitatively described by applying the pseudo phase approximation, PPA, with quadratic and cubic terms in the excess free energy of mixing, G_e , included for both the surface and micelle mixing. The pseudo phase approximation means that at equilibrium the chemical potential of the components of the pseudo phases, micelles, surface and solution monomer, are equal. Equating the chemical potentials of the micelle and monomer gives (47, 48),

$$x_i = \frac{c_i^{mon}}{f_i^m c_i^\mu} \quad (4)$$

where x_i is the mole fraction of the i^{th} component in the micelle, c_i^{mon} the monomer concentration of the i^{th} component, f_i^m its activity coefficient in the micelle, and c_i^μ its cmc. For a binary mixture, assuming the micelle mole fractions equal unity and at the cmc $c_i^{mon} = \alpha_i c_i^{mix}$, where α_i is the mole fraction of monomer in solution and c_{mix}^μ the mixed cmc,

$$\frac{1}{c_{mix}^\mu} = \frac{\alpha_1}{f_1 c_1^\mu} + \frac{\alpha_2}{f_2 c_2^\mu} \quad (5)$$

Here the activity coefficients are derived from an expansion of the excess free energy of mixing, G_e , which includes quadratic and cubic terms (47, 48),

$$G_e = x_1 x_2 \beta_{12} + x_1 x_2 (x_1 - x_2) C_{12} \quad (6)$$

where B_{12} and C_{12} are the interaction constants. $B_{12}=C_{12}=0$ represents ideal mixing. In the Regular Solution Approximation, RST, C_{12} is zero, and represents in that case an interaction which is symmetrical with the solution composition. A non-zero cubic term allows for asymmetry in the interaction. In this paper the interaction constant B_{12} and C_{12} are abbreviated to B and C , and the subscripts m and s refer to the micelle and surface. In general a negative interaction constant implies an attractive synergistic interaction, whereas a positive interaction constant is consistent with a repulsive interaction.

As described in detail elsewhere (49, 50) this leads to a set of equations that can be solved iteratively to obtain the cmc variation, the variations in micelle compositions and the variation in surface and monomer concentrations below and above the cmc.

RESULTS and DISCUSSION

(i) Surface tension data

The variation in surface tension with concentration is shown in figure S1 of Supporting Information, and the surface tension shows a strong dependence upon the solution composition.

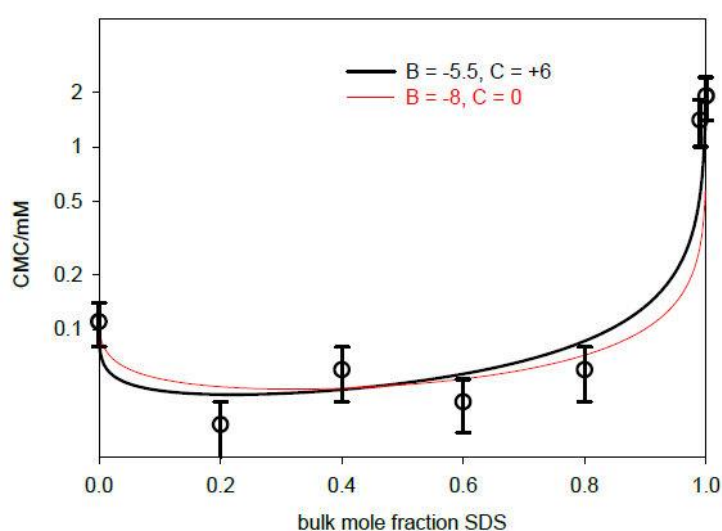


Figure 2. Variation in cmc for escin / SDS mixtures in 0.1 M NaCl. The solid black line is a calculation using equation 5 for $B_m = -5.5$, and $C_m = +6.0$, and the red line is for a regular solution application for $B_m = -8$, see also legend for details.

The mixed cmc values are derived from the inflexion points of the ST curves, and along with the ST values above the cmc are summarised in table S1 in the Supporting Information. The variation in the cmc is plotted in figure 2. The cmc value obtained from the data for SDS of 1.9 mM is in relatively good agreement with literature values (53), and for escin is close to that previously reported (39), ~ 0.1 mM. Without any quantitative analysis it is clear that there is a considerable reduction in the cmc for the escin / SDS mixtures. This indicates that there is a significant attractive interaction between the escin and the SDS in solution, and that the mixing is highly non-ideal. Furthermore the behaviour indicates a very favourable mixing in the solution aggregates.

The lines in figure 2 are from the pseudo phase approximation, equation 5, for activity coefficients defined in equation 6. The red line is for the regular solution approximation, in which the cubic term, C_m , is zero, and for a quadratic symmetrical term, B_m , of -8.0. The solid black line, which gives a marginally better description, is for activity coefficients which include the quadratic and cubic terms in equation 6; for $B_m=-5.5$ and $C_m=+6.0$. It has been previously observed that the cmc variation is not particularly sensitive to the higher order terms in the expansion of the free energy of mixing (50-52), and either analysis is equally acceptable description of the cmc variation. However, in the subsequent analysis of the variation in the surface composition it will be seen that the asymmetry introduced by the cubic term is both important and essential to describe the solution and the surface mixing

(ii) Escin / SDS adsorption

The escin / SDS mixed adsorption at the air-water interface was measured by NR at two fixed total surfactant concentrations of 0.3 and 1.5 mM, and variable solution compositions. Apart from solutions rich in SDS, the solutions at 0.3 and 1.5 mM are both above the mixed cmc over most of the composition range studied, by an average factor of x5 and x25 respectively. Further complementary measurements were made at a fixed composition of 50 / 50 mole ratio and variable solution concentrations from 0.3 to 1.5 mM. At each point measurements were made for the isotopic combinations of d-SDS / escin and h-SDS / escin in nrw. Some representative NR data are shown in figure 2 for 0.3 mM SDS / escin at a solution mole ratio of 80/20.

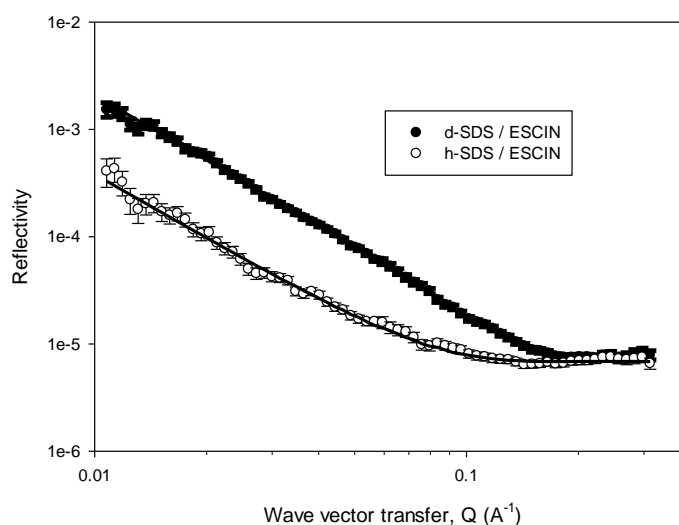
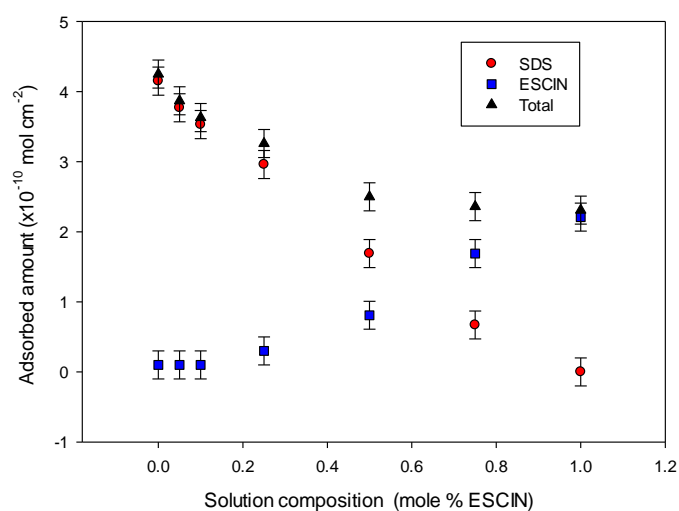


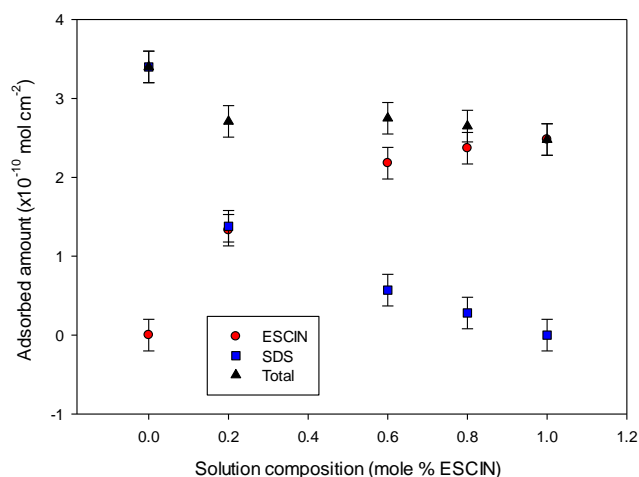
Figure 3. NR data for 80/20 mole ratio SDS / escin at a solution concentration of 0.3 mM; (o) d-SDS / escin, (●) h-SDS / escin. The solid lines are model calculations for a single uniform layer at the interface, as described in the text.

The NR data shown in figure 3 are well described as a single monolayer of uniform composition, and evaluated using equation 1 to obtain a layer thickness, d , and a scattering length density, ρ . For d-SDS / escin and h-SDS / escin data in figure 3 the values of d and ρ are 26 Å, $1.43 \times 10^{-6} \text{ Å}^{-3}$, and 27 Å, $0.57 \times 10^{-6} \text{ Å}^{-3}$ respectively. In terms of the calculation of the adsorbed amount (using equation 3) it is the product $d \cdot \rho$ which is important, and are 3.72 and $1.55 \times 10^{-5} \text{ Å}^{-2}$ respectively. The corresponding area/molecule and adsorbed amounts for the data in figure 3 are then for the SDS and escin 120, 125 Å², and 1.38, $1.33 \times 10^{-10} \text{ mol cm}^{-2}$. Typical errors in the adsorbed amounts are $\sim \pm 0.2 \times 10^{-10} \text{ mol cm}^{-2}$, and in the surface composition ~ 0.02 in mole fraction.

The variation in adsorbed amount is shown in figure 4a and surface composition in figure 5b for 1.5 mM SDS / escin. The key model parameters are summarised in table 2.



(a)



(b)

Figure 4. Adsorbed amount versus solution composition (mole fraction escin), (a) 1.5 mM SDS / escin in 0.1 M NaCl, (b) 0.3 mM SDS / escin in 0.1 M NaCl, see legend for details.

Table 2. Key parameters for the adsorption of 1.5 mM SDS / escin in 0.1 M NaCl

SDS/escin solution mole ratio	SDS		Escin		$\Gamma_{\text{total}} (\times 10^{-10} \text{ mol cm}^{-2})$	Surface mole % escin (± 0.02)
	A ($\pm 2 \text{ \AA}^2$)	$\Gamma (\pm 0.2 \times 10^{-10} \text{ mol cm}^{-2})$	A	Γ		
100/0	40	4.15	-	-	4.15	<0.05
95/5	44	3.77	-	-	3.77	<0.05
90/10	47	3.53	-	-	3.53	<0.05
75/25	56	2.96	>400	<0.3	3.00	<0.1
50/50	98 (± 5)	1.69	205 (± 10)	0.81	2.5	0.32
25/75	248 (± 10)	0.67	98 (± 5)	1.69	2.36	0.72
0/100	-	-	75	2.21	2.21	1.0

The data in figure 4a and table 2 show that at a solution concentration of 1.5 mM and for solutions rich in SDS the SDS totally dominates the adsorption. For solution compositions, SDS / escin, from 100/0 to 90/10 mole ratio, there is (within the sensitivity of the method) essentially no escin adsorption measurable at the interface. As the solution becomes richer in escin the amount of escin adsorption increases, such that at 60 mole% escin in solution the amounts of SDS and escin at the interface are equivalent. The total adsorption and the adsorbed amounts of the individual components reflect the saturated adsorption of the corresponding pure components; and this is almost a factor 2 higher for SDS than for escin. The cmc of escin is significantly lower than that for SDS, and this implies a greater surface activity for escin. However the saturation adsorbed amounts are quite different and are much higher for SDS than

for escin due to the different packing constraints. The variation in the surface composition is shown in figure 5b, and the SDS adsorption (as a mole fraction) dominates the adsorption over much of the composition range studied. The surface mixing is highly non-ideal. The data are consistent with the application of the pseudo phase approximation, with the inclusion of quadratic and cubic terms in the expansion of the non-ideal activity coefficients (50, 51), and the key parameters are summarised in table 3.

TABLE 3. *Summary of non-ideal PPA model parameters for SDS / escin in 0.1 M NaCl*

B_s	C_s	x_{bc}	G_{emin} (BC)
-2.0	+2.2	0.3	-0.70

The equivalent parameters for the micelle mixing are $B_m = -5.5$, $C_m = +6.0$ and $G_e \sim -2.0$ kT. x_{bc} is the mole fraction of SDS in the surface at the minimum in the excess free energy of mixing.

Equivalent adsorption and composition data at a total surfactant concentration of 0.3 mM are shown in figures 4b and 5a, and the key model parameters are summarised in table 4.

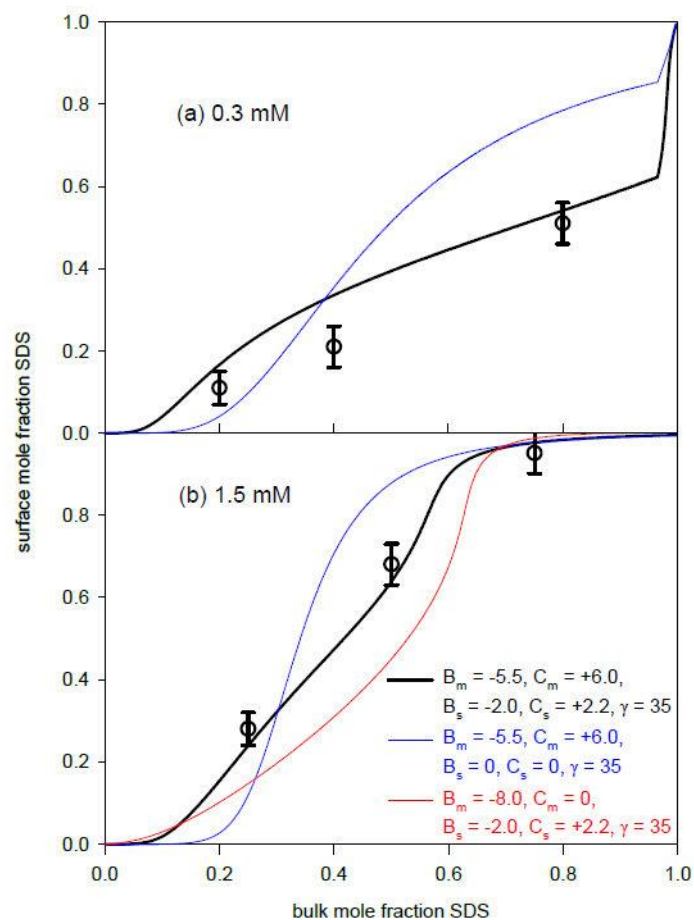


Figure 5. Variation in surface composition (mole fraction SDS) with solution composition for SDS / escin / 0.1 M NaCl (a) 0.3 mM, (b) 1.5 mM. The solid black line is a calculated curves based on the pseudo phase approximation (as described in the text), using the model parameters summarised in table 3, the blue line is for ideal surface mixing and the red line is for a non-ideal regular solution micelle mixing; see also legend for details.

Table 4. Key parameters for the adsorption of 0.3 mM SDS / escin in 0.1 M NaCl

SDS/escin solution mole ratio	SDS		escin		$\Gamma_{\text{total}} (\times 10^{-10}$ mol cm ⁻²)	Surface mole % escin (± 0.02)
	A ($\pm 2 \text{ \AA}^2$)	$\Gamma (\pm 0.2 \times 10^{-10}$ mol cm ⁻²)	A	Γ		
0/100	-	-	67	2.48	2.48	1.0

20/80	593 (± 25)	0.28	70	2.37	2.65	0.89
40/60	293(± 10)	0.57	76	2.18	2.75	0.79
82/20	120(± 5)	1.38	125	1.33	2.71	0.49
100/0	50	3.40	-	-	3.40	0.0

Broadly similar trends are observed in the adsorption data in figure 4b and table 4 at a total surfactant concentration of 0.3 mM compared to that measured at 1.5 mM (see figure 4a and table 2). However, in detail the variation in adsorption and surface composition are different. Although at the surfactant concentration of 0.3 mM the mixtures are also above the cmc over most of the composition range, they are much closer to the cmc. In this case the adsorption, as measured across the solution composition range, is more dominated by the escin adsorption. The variation in the surface composition, see figure 5a, is now more reflecting the greater surface activity of the escin compared to the SDS, as indicated by the relative cmc values. The solid lines in figure 5a are for model calculations of non-ideal mixing using the Pseudo phase approximation as described earlier. However, importantly the variation in the surface composition are described using the same key model parameters as summarised in table 3. In both figures 5 a and b the blue line is a calculation for ideal surface mixing. This gives an indication of the extent to which the surface departs from ideal mixing.

NR measurements were also made for a SDS / escin mixture at a fixed SDS / escin mole ratio of 50/50 and variable surfactant concentrations from 0.3 to 1.5 mM. The data are shown and summarised in figure S2 and table S2 in the Supporting Information. The variation in surface composition with solution concentration is shown in figure 6. The results show a gradual transition from a surface dominated by escin to one dominated by SDS, as the surfactant concentration increases from close to the cmc to well above the cmc. The solid black line in figure 6 is the calculated variation in the surface composition from the pseudo phase approximation, using the same quadratic and cubic terms, B_s and C_s , in the expansion of the excess free energy of mixing as used in figure 5 (see table 5) at a fixed surfactant concentration and variable composition.

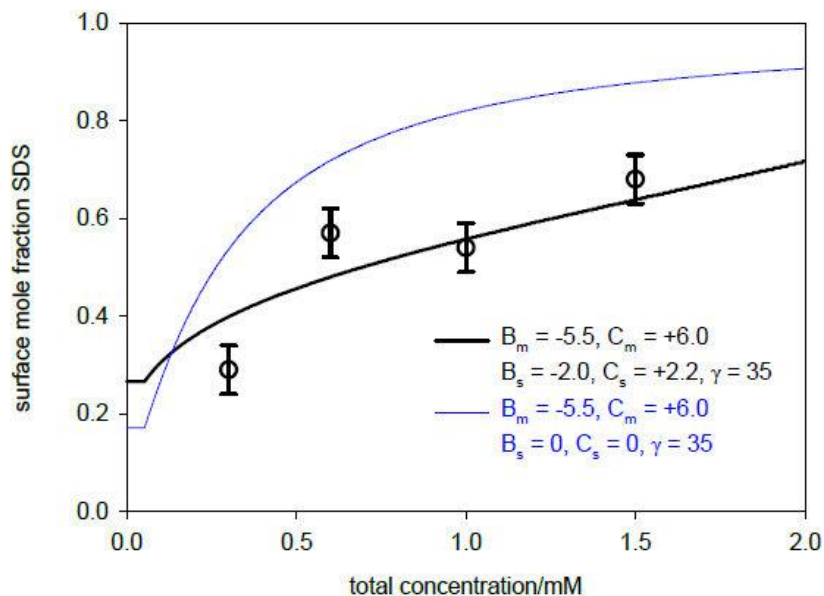


Figure 6. Variation in surface composition (mole fraction SDS) with solution concentration for 50/50 mole ratio SDS / escin / 0.1 M NaCl. The solid black line is a calculated curves based on the pseudo phase approximation (as described in the text), using the model parameters summarised in table 3, and the blue line is for ideal surface mixing; see also legend for details.

The blue solid line again corresponds to a calculation using ideal surface mixing, and gives an indication of the degree to which the surface mixing departs from the ideal. The short horizontal region in the calculated curves at very low surfactant concentrations correspond to the region where the total concentration drops below the mixed cmc. It is also notable that the deviations between the data and the calculated curves are greatest at the lower surfactant concentration. As the cmc is approached there will be a greater polydispersity in the micelle composition and size and this will impact increasingly upon the free monomer composition and concentration which drives the adsorption. This is not accounted for in the application of the pseudo phase approximation here.

In the development of formulations involving natural components it is often a requirement to minimise the amount of the more expensive components, in this case the saponin. Hence it is instructive to be able to follow the surface mixing at a fixed low saponin concentration as a function of surfactant concentration. This has been done here and NR measurements were also made for the SDS / escin mixture at a fixed escin concentration of 0.01 wt% ($9 \times 10^{-5} \text{M}$) and variable SDS concentrations. In this case the solution composition and concentration are both

changing. The adsorbed amounts and surface composition are plotted as a function of SDS concentration in figure 7, and the key parameters are summarised in table 5.

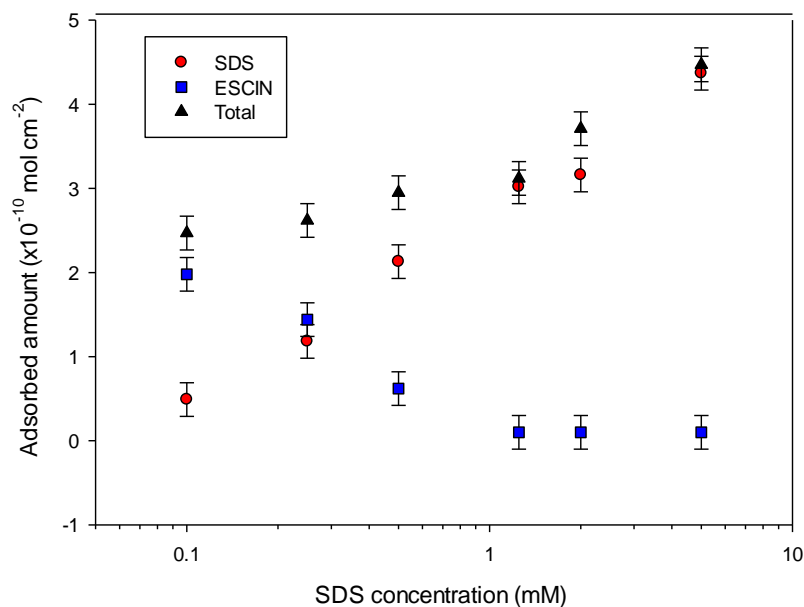


Figure 7. Adsorbed amount versus SDS concentration for SDS / 0.01 wt% (9×10^{-5} M) escin in 0.1 M NaCl, see legend for details.

Table 5. Key parameters for 0.01 wt% (9×10^{-5} M) escin / SDS in 0.1 M NaCl adsorption

SDS concentration (mM)	Total concentration (M)	Solution composition (mole% ESCIN)	SDS		escin		Γ_{total} ($\pm 0.2 \times 10^{-10}$ mol cm ⁻²)	Surface mole % escin (± 0.02)
			A ($\pm 2 \text{ \AA}^2$)	Γ ($\pm 0.2 \times 10^{-10}$ mol cm ⁻²)	A	Γ		
5.0	5.09×10^{-3}	0.02	38	4.37	-	-	4.37	<0.05
2.0	2.09×10^{-3}	0.04	46	3.61	-	-	3.61	<0.05
1.25	1.34×10^{-3}	0.07	55	3.02	-	-	3.02	<0.05
0.5	5.9×10^{-4}	0.15	78	2.13	267	0.62	2.95	0.17
0.25	3.4×10^{-4}	0.26	141 (± 5)	1.18	115	1.44	2.62	0.55
0.1	1.9×10^{-4}	0.47	347 (± 15)	0.49	84	1.98	2.47	0.80

Consistent with the results in figure 4 and 5 the surface adsorption is dominated by escin at the lower SDS concentrations, whereas at the higher SDS concentrations the surface is dominated by the SDS adsorption. As illustrated in table 5, as the SDS concentration increases the solution

composition is increasingly dominated by the SDS, where the total SDS concentration increases from 0.2 to ~ 5 mM.

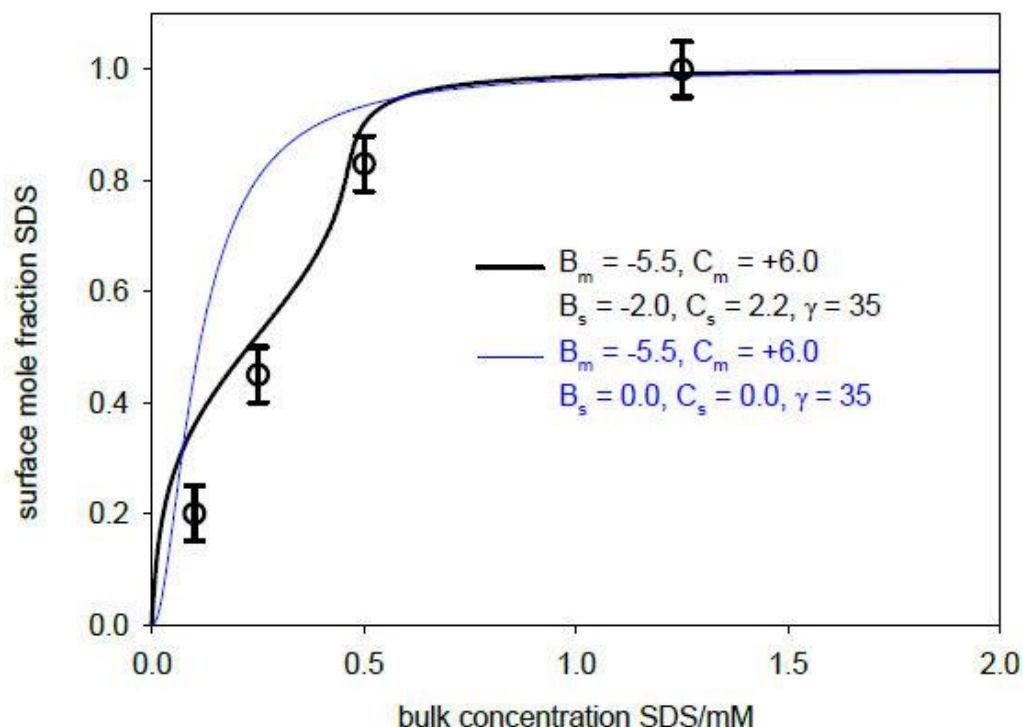


Figure 8. Variation in surface composition (mole fraction SDS) with SDS concentration for SDS / 0.01 wt% (9×10^{-5} M) escin / 0.1 M NaCl. The solid black line is a calculated curves based on the pseudo phase approximation (as described in the text), using the model parameters summarised in table 3, and the blue line is for ideal surface mixing; see also legend for details.

In figure 8 the variation in the surface composition (mole fraction SDS) versus the SDS concentration is plotted. The data show a rather different form to that presented in figure 6. As shown in table 5 both the total concentration and composition are varying over the concentration range studied. The solution composition, as a mole fraction of escin, varies from 0.47 at the lowest SDS concentration to 0.02 at the highest SDS concentration. As the surface is already dominated by the SDS at an SDS concentration of 1.25 mM, the data in table 5 for SDS concentrations > 1.25 mM are not included in the figure. The blue line in the figure is for ideal surface mixing and again shows the extent to which the surface departs from ideal mixing. The solid black line is the pseudo phase approximation calculation using the B_s and C_s terms

in the excess free energy of mixing with the same values as used for all the previously presented adsorption data (see table 3).

The variation in surface composition with solution composition for SDS / escin in 0.1 M NaCl at surfactant concentrations of 0.3 and 1.5 mM and the variations with varying surfactant concentration at variable and fixed compositions are all well described by the pseudo phase approximation in which the quadratic (B_s) and cubic (C_s) terms are included in the expansion of the excess free energy of mixing. The attractive interaction is characterised by the same micelle and surface parameters in all the cases analysed here. The blue lines in figures 5 a and b are for ideal surface mixing and the intersection between that and the curve (solid black line) for non-ideal mixing corresponds to the compositions at which the excess free energy of mixing is at a minimum (50-52). This corresponds to a surface composition of 0.3 (mole fraction of SDS) at surfactant concentrations of 1.5 mM and 0.3 mM. The data and calculations in figures 5, 6 and 8, at varying surfactant concentration, are also consistent with the minimum in the free energy of mixing occurring at a surface composition of 0.3 mole fraction SDS. That is, the surface mixing is highly asymmetrical. In the regular solution approach (in which C_s is zero) the minimum in the excess free energy of mixing is at a surface composition of 0.5. The asymmetry in the interaction between the two surfactants could be expected to arise from the electrostatic interactions and from differences in packing criteria, steric effects. In an ordered 2-D mixture of charged and uncharged components the simplest arrangement that minimises repulsion for the highest mixing ratio is 2:1 nonionic / ionic. Hence the minimum in the excess free energy of mixing, G_e , occurs at a mole fraction of SDS ~ 0.3 , and is consistent with that arrangement, as discussed by Patist et al (54) and Reif and Somasundaran (55). However, given that the measurements are made in 0.1 M NaCl it might be expected that the electrostatic interactions are substantially reduced. From the molecular structure of escin compared to SDS (see figure 1), it might be expected that there is also a significant contribution from steric or packing effects at the interface.

From the ST data the variation in cmc with solution composition were analysed using equation 5 to characterise the nature of the micelle mixing. It was observed that the cmc data were not so sensitive to the asymmetry of the excess free energy of mixing and that the data could be fitted equally well using the symmetrical regular solution approach, of $B_m=-8.0$, and $C_m=0.0$, and from the asymmetrical form including the quadratic and cubic terms in the expansion of G_e , of $B_m=-5.5$, and $C_m=+6.0$. However, the surface mixing is much more sensitive to the form of the micelle mixing. Using the regular solution form of the micelle mixing it was not possible

to reproduce the surface mixing at either of the surfactant concentrations, 0.3 and 1.5 mM, as clearly illustrated in figure 5b, where the red curve is a calculation for same surface parameters but the RST micelle parameters, and the asymmetrical form with $B_m = -5.5$, and $C_m = +6.0$ was required. The micelle mixing determines the free monomer composition and concentration in equilibrium with the micelle phase, and it is the monomer concentration that drives the surface adsorption. Hence the implication here is that the asymmetry in the surface mixing is dictated by the monomer composition, which in turn is determined by the micellar phase. This implies here that over much of the composition range the micelles are relatively rich in escin and the monomer is correspondingly depleted of escin.

It is also notable, when comparing the non-ideality parameters, B , and C , and the minimum excess free energy of mixing, G_e , between the surface and the micelles, that there is a stronger attractive interaction between the escin and SDS in the micelles compared to the surface. In terms of the excess free energy of mixing it is ~ -2 kT in the micellar phase and ~ -0.7 kT for surface mixing. Although it is not unusual or unexpected that the surface and micelle interactions are different, in the presence of electrolyte the differences in mixed anionic – nonionic surfactant mixtures are usually quite small (56). This implies that micelle formation is more energetically favourable than surface adsorption, as a result of greater steric or packing constraints at the surface compared to in the micelles. It is not perhaps surprising that the extra degrees of freedom associated with the micelle structures enables the packing constraints to be less severe in the micelles than at the surface. However, in spite the presence of 0.1 M NaCl which must substantially reduce the electrostatic contribution, the micelle interaction is unusually strong. This further reinforces the supposition that the main contribution to the interaction between the escin and SDS is steric.

(iii) Discussion

The ST and NR results show that the mixing of escin and SDS in micelles and at the surface is highly non-ideal, even in the presence of 0.1 M NaCl. Furthermore the surface mixing is highly asymmetric and requires the addition of quadratic and cubic terms in the expansion of the excess free energy of mixing to reproduce the trends in the adsorption data. The minimum in the excess free energy of mixing at the surface occurs at a surface mole fraction of SDS ~ 0.3 . This is consistent with the ideal packing for nonionic-ionic mixtures in 2-D to minimise electrostatic interactions of 2:1, as observed in related systems (50-52, 54, 55). The impact of the relative contributions to the excess free energy of mixing from electrostatic interactions,

steric or packing effects and changes in hydration, have been discussed at length elsewhere (50-52), and they can all contribute significantly to the asymmetry in mixing (51, 52). In the study of the ternary surfactant mixture of C₁₂E₈ / LAS / SLES Liley et al (51, 52) were able to qualitatively identify the relative contributions due to electrostatic interactions and steric effects by making measurements with and without electrolyte. This was not done here as the interest was in the behaviour of SDS / escin mixture in the presence of electrolyte. However the significant difference in the departure from ideality in the micelle mixing obtained from the cmc data, the surface mixing obtained from the NR data, and the presence of electrolyte which reduces the impact of the electrostatic interactions, suggest that the asymmetry in the mixing is due to both electrostatic and steric effects.

The relative importance of the steric contribution is highlighted by the difference in the non-ideality parameters for the surface and micelle. The micelle mixing is significantly more non-ideal. That is, there is a more attractive interaction between the escin and SDS in the micelles than at the surface. This implies that the packing constraints are more severe at the surface compared to the micelles. Although differences in the surface and micelle parameters are often encountered in the regular solution approach (56) and in the application of the pseudo phase approximation including quadratic and cubic terms (50-52) they are not usually as large as those reported here.

The surface adsorption properties of SDS / escin mixtures in 0.1 M NaCl have been studied under a wide range of conditions: by varying the solution composition at fixed surfactant concentrations of 0.3 and 1.5 mM; at a fixed solution composition, equimolar, and a variable concentration; and by varying the solution composition and concentration simultaneously. It is difficult a priori to decide which range of compositions and concentrations will provide the most sensitive test of theory. However given the wide range of solution conditions studied here it is important to observe that all the data can be adequately described by a single set of pseudo phase approximation model parameters. It is also important to observe that the strong micellar interaction, which arises from the cmc variation, is required in order to understand the nature of the surface mixing. However the cmc data provides little information about the micelle compositions, and this comes, as discussed earlier, predominantly from the adsorption data and especially from the data at the solution concentration of 1.5 mM.

CONCLUSIONS

Penfold et al (39) have previously characterised the adsorption of the saponin escin by NR, and related the unusual surface rheology that has been reported (12-17) to the structure of the adsorbed layer. In the context of a wider range of applications and potential applications (1-10) it is likely that saponins will be formulated with different synthetic surfactants. Here NR has been used to characterise the adsorption of escin with the anionic surfactant SDS at the air-water interface. The results provide a basis for understanding the mixing behaviour of saponin / surfactant mixtures and the role of their relative surface activities. The surface mixing is shown to be highly non-ideal and the mixing has been characterised quantitatively using the recent development of the pseudo phase approximation in which both the quadratic and cubic terms in the expansion of the excess free energy of mixing are included (50-52). The asymmetry in the surface composition and the excess free energy of mixing, accounted for by the inclusion of the cubic term, is attributed to contributions from both electrostatic interactions and steric interactions, with the interaction being dominated by a steric contribution.

ACKNOWLEDGEMENTS

The provision of beam time on the SURF and INTER reflectometers at ISIS is acknowledged. The invaluable scientific and technical assistance of the Instrument Scientists and support staff is greatly appreciated. IMT, REP, AB and SLH thank Innovate UK for funding under the IB catalyst scheme grant no 131168 “A synthetic biology-based approach to engineering triterpenoid saponins and optimisation for industrial applications”

SUPPORTING INFORMATION

Some additional data, in the form of tables and figures are available in the Supporting Information.

AUTHOR INFORMATION

Corresponding author: Jeff Penfold, jeff.penfold@stfc.ac.uk

Author Contributions: All Authors have given their approval for the final version of the manuscript

Funding Sources: Funded through the beam time awarded at the STFC’s ISIS Facility, and funding from Innovate UK under the IB catalyst scheme, grant no 131168 “A synthetic biology-based approach to engineering triterpenoid saponins and optimisation for industrial applications”

REFERENCES

- (1) Oakenfull, D. Saponins in food – a review. *Food Chemistry*, **1991**, 6, 19-40
- (2) Sparg, S. G.; Light, M. E.; van Staden, J. Biological activities and distribution of plant saponins. *J. Ethnopharmacology*, **2004**, 94, 219-242
- (3) Vinken, J. P.; Heng, L.; de Groot, A.; Gruppen, H. Saponins: classification and occurrence in the plant kingdom. *Phytochemistry*, **2007**, 68, 275-297
- (4) Guclu-Ustundag, O.; Mazza, G. Saponins: properties, applications, and processing, *Critical Rev. Food Science and Nutrition*, **2007**, 47, 231-258
- (5) Hoslettmann, K.; Marstom, A. Saponins, *Cambridge University Press*, NY, **1995**
- (6) Cheeke, P.R. Actual and potential applications of Yucca Schidigera and Quillaja Saponana saponins in human and animal nutrition, *Proc. Am. Soc. Anim. Sci.* **1999**, E9, 1-10
- (7) Jenkin, K. J.; Atwal, A. S. Effects of dietary saponins on fecal bile acids and neutral steroids and availability of vitamin A and E in the chick, *J. Nutr. Biochem.* **1994**, 5, 134-137
- (8) Liu, J.; Henkel, T. Traditional Chinese medicine: are polyphenols and saponins the key ingredients triggering biological activity, *Curr. Med. Chem.* **2002**, 9, 1483-1485
- (9) Fukuda, N.; Tanaka, H.; Shoyawa, Y. Isolation of pharmacologically active saponin Ginsenoside Rb1 from Ginseng by immunoaffinity column chromatography, *J. Nat. Prod.* **2000**, 62, 283-285
- (10) Brown, R. The natural way in cosmetics and skin care, *Chem. Mark. Rep.* **1998**, 254, FR8
- (11) Sirtori, C. R. Aescin: pharmacology, pharmacokinetics and therapeutic profile, *Pharmacol. Res.* **2001**, 44, 183-193
- (12) Van Wazer, J. Some rheological measurements on the surface of saponin in water, *J. Coll. Sci.* **1947**, 2, 223-231
- (13) Stanimirova, R.; Marinova, K.; Tcholakova, S.; Denkov, N. D.; Stoyanov, S. D.; Pelan, E. Surface rheology of saponin adsorption layers, *Langmuir*, **2011**, 27, 12486-12498

- (14) Golemanov, K.; Tcholakova, S.; Denkov, N. D.; Pelan, E.; Stoyanov, S. D. Surface shear rheology of saponin adsorbed layers, *Langmuir*, **2012**, 28, 12071-12084
- (15) Wojciechowski, K. Surface activity of saponin from Quillaja bark at the air/water and oil/water interfaces, *Coll. Surf. B*, **2013**, 108, 95-102
- (16) Golemanov, K.; Tcholakova, S.; Denkov, N. D.; Pelan, E.; Stoyanov, S. D. Remarkably high surface visco-elasticity of adsorption layers of triterpenoid saponins, *Soft Matter*, **2013**, 9, 5738-5752
- (17) Golemanov, K.; Tcholakova, S.; Denkov, N. D.; Pelan, E.; Stoyanov, S. D. The role of the hydrophobic phase in the unique rheological properties of saponin adsorbed layers, *Soft Matter*, **2014**, 10, 7034-7044
- (18) Wojciechowski, K.; Orczyk, M.; Marcinkowski, K.; Kobiela, T.; Trapp, M.; Gutberlet, T.; Geue, T. Effect of hydration of sugar groups on adsorption of Quillaja bark saponin at the air-water and Si/water interfaces, *Coll. Surf. B*, **2014**, 117, 60-67
- (19) Pagureva, N.; Tcholakova, S.; Golemanov, K.; Denkov, N. D.; Pelan, E.; Stoyanov, S. D. Surface properties of adsorption layers formed from triterpenoid and steroid saponins, *Coll. Surf. A*, **2016**, 491, 18-28
- (20) Bottcher, S.; Drusch, S. Interfacial properties of saponin extracts and their impact in foam characterisation, *Food Biophysics*, **2016**, 11, 91-100
- (21) Tippel, J.; Lehmann, M.; von Klitzing, R.; Drusch, S. Interfacial properties of Quillaja saponins and its use for micellisation of lutein esters, *Food chemistry*, **2016**, 212, 35-42
- (22) Mitra, S.; Dungan, S.R. Micellar properties of Quillaja saponin. 1. Effect of temperature, salt and pH on solution properties, *J. Agric. Food Chem.* **1997**, 45, 1587-1595
- (23) Mitra, S.; Dungan, S. R. Micellar properties of Quillaja saponins, 2. Effect of solubilised cholesterol on solution properties, *Coll. Surf. B*, **2000**, 17, 117-133
- (24) Mitra, S.; Dungan, S. R. Cholesterol solubilisation in aqueous micellar solutions of Quillaja saponin, bile salts or nonionic surfactants, *J. Agric. Food Chem*, **2001**, 49, 384-394
- (25) Tykaraska, E.; Sobiak, S.; Gdaniec, M. Supramolecular organisation of neutral and ionic forms of pharmaceutically relevant Glycyrrhizic acid – amphiphile self-assembly and inclusion of small drug molecules, *Cryst. Growth Res.* **2012**, 12, 2133-2137

- (26) Kitamoto, D.; Morita, T.; Fuluota, T.; Kinishi, M.A.; Imura, T. Self-assembly properties of glycolipid biosurfactant and their potential applications, *Curr. Opin. Coll. Int. Sci.* **2009**, 14, 315-328
- (27) Peixto, M. P. G.; Treter, J.; de Reseudo, P.E.; de Silveira, N. O.; Ortega, G. G.; Lawrence, M. J.; Driess, C. A. Wormlike micelles aggregates of Saponins from the Paraguariensis A St Hil (mate): a characterisation by cryo-TEM, rheology, light scattering, and small angle neutron scattering, *J. Pharmaceutical Sci.* **2011**, 100, 536-546
- (28) Liu, J.; Harms, M.; Garamus, V. M.; Muller-Goynam, C. C. Reentrant structural phase transition in amphiphilic self-assembly, *Soft Matter*, 2013, 9, 6371-6375
- (29) Wojciechowski, K.; Orczyk, M.; Gutberlet, T.; Geue, T. Complexation of phospholipids and cholesterol by triterpene saponins in bulk and in monolayers, *Biochimica et Biophysica Acta*, **2016**, 1858, 363-373
- (30) Matsuoka, K.; Miyajima, R.; Ishida, Y.; Karasawa, S.; Yoshimura, T. Aggregate formation of glycyrrhizic acid, *Coll. Surf. A*, **2016**, 500, 112-117
- (31) Wojciechowski, K.; Piotrowski, M.; Popielarz, W.; Sesnowski, T. R. Short and mid-term adsorption behaviour of Quillaja Bark Saponin and its mixtures with Lysozyme, *Food Hydrocolloids*, **2011**, 25, 687-693
- (32) Piotrowski, M.; Lewandoski, J.; Wojciechowski, K. Biosurfactant – protein mixtures: Quillaja Bark Saponin at water/air and water/oil interfaces, in the presence of β -lactoglobulin, *J. Phys. Chem. B*, **2012**, 116, 4843-4850
- (33) Kerwon, A.; Wojciechowski, K. Interaction of Quillaja Bark Saponin with food relevant proteins, *Adv. Coll. Int. Sci.* **2014**, 209, 185-195
- (34) Wojciechowski, K.; Kerwon, A.; Lewandowska, J.; Marcinkowski, K. Effect of β -casein on surface activity of Quillaja Bark Saponin at fluid-fluid interfaces, *Food Hydrocolloids*, **2014**, 24, 208-216
- (35) Bottcher, S.; Scampechio, M.; Drusch, S. Mixtures of saponins and β -lactoglobulin differ from classical protein/surfactant systems at the air-water interface, *Coll. Surf. A*, **2016**, 506, 765-773
- (36) Wojciechowski, K.; Orczyk, M.; Gutberlet, T.; Trapp, M.; Marcinkowski, K.; Kobiak, T.; Geue, T. Unusual penetration of phospholipid mono and bilayers by Quillaja Bark Saponin biosurfactant, *Biochimica et Biophysica Acta*, **2014**, 1838, 1931-1940

- (37) Jian, H. L.; Liao, X. X.; Zhu, L. W.; Zhang, W. M.; Jiang, J. X. Synergism and foaming properties in binary mixtures of a biosurfactant derived from *Camellia Oleifera* Able with synthetic surfactants, *J. Coll. Int. Sci.* **2011**, 359, 487-492
- (38) Reichart, C. I.; Salminen, H.; Bonisch, C. B.; Schaefer, C.; Weiss, J. Concentration effect of Quillaja saponin-cosurfactant mixtures on emulsifying properties, *J. Coll. Int. Sci.* **2018**, 519, 71-80
- (39) Penfold, J.; Thomas, R. K.; Tucker, I.; Petkov, J. T.; Stoyanov, S. D.; Denkov, N. D.; Golemanov, K.; Tcholakova, S.; Webster, J. R. P. Saponin adsorption at the air-water interface-neutron reflectivity and surface tension study, *Langmuir*, **2018**, 34, 9540-9547
- (40) Tsibranska, S.; Ivanova, A.; Tcholakova, S.; Denkov, N. D. Self-assembly of ESCIN molecules at the air-water interface as studied by molecular dynamics, *Langmuir*, **2017**, 33, 8330-8341
- (41) Lu, J. R.; Thomas, R. K.; Penfold, J. Surfactant layers at the air-water interface: structure and composition, *Adv. Coll. Int. Sci.* **2000**, 84, 143-304
- (42) Penfold, J.; Thomas, R. K. Mixed surfactants at the air-water interface, *Ann. Rep. Prog. Chem. Section C*, **2010**, 106, 14-35
- (43) Penfold, J.; Thomas, R. K. The limitations of models of surfactant mixing at interfaces, as revealed by neutron scattering, *PCCP*, **2013**, 15, 7017-7027
- (44) Webster, J.; Holt, S.; Dalgleish, R. INTER: the chemical interfaces reflectometer on target station 2 at ISIS, *Physica B*, **2006**, 385-386, 1164-1166
- (45) Penfold, J. et al, Recent advances in the study of chemical surfaces and interfaces by specular neutron reflection, *J. Chem. Soc. Faraday Trans.* **1997**, 93, 3899-3917
- (46) Lu, J. R.; Morrocco, A.; Su, T. J.; Thomas, R. K.; Penfold, J. Adsorption of dodecyl sulfate surfactants with monovalent metal counterions at the air-water interface, studied by neutron reflection and surface tension measurements, *J. Coll. Int. Sci.* **1993**, 158, 303-316
- (47) Rubingh, D. N. in *Solution chemistry of Surfactants*, Ed Mittal K. L. *Plenum Press*, NY, **1979**, pp 337-354
- (48) Holland, P. M. Nonideal mixed micelle solutions, *Adv. Coll. Int. Sci.* **1986**, 26, 111-129
- (49) Holland, P. M.; Rubnigh, D. N. Nonideal multicomponent mixed micelle model, *J Phys. Chem*, **1983**, 87, 1984-1990

- (50) Li, P. X.; Ma, K.; Thomas, R. K.; Penfold, J. Analysis of the asymmetric synergy in the adsorption of zwitterionic-ionic surfactant mixtures at the air-water interface below and above the cmc, *J. Phys. Chem. B* **2016**, 120, 3677-3691
- (51) Liley, J.; Thomas, R. K.; Penfold, J.; Tucker, I. M.; Petkov, J. T.; Stevenson, P.; Webster, J. R. P. Surfactant adsorption in ternary surfactant mixtures above the cmc: the importance of the shape of the excess free energy, *J Phys Chem B*, **2017**, 121, 2825-2838
- (52) Liley, J.; Thomas, R. K.; Penfold, J.; Tucker, I. M.; Petkov, J. T.; Stevenson, P.; Webster, J. R. P. The impact of electrolyte on the adsorption at the air-water interface for a ternary surfactant mixture above the cmc, *Langmuir*, **2017**, 33, 4301-4312
- (53) van Os, N. M.; Haak, J. R.; Rupert, L. A. M. Physico-chemical properties of selected anionic, cationic and nonionic surfactants, *Elsevier*, Amsterdam, **1993**
- (54) Patist, A.; Dev, S.; Shah, D.O.; Importance of 1:3 molecular ratio on the interfacial properties of mixed surfactant systems, *Langmuir*, **1999**, 15, 7403-7405
- (55) Reif, I.; Somasundaran, P. Asymmetric excess free energies and variable interaction parameters in mixed micellisation, *Langmuir*, **1999**, 15, 3411-3417
- (56) Staples, E.; Thompson, L.; Tucker, I.; Penfold, J.; Thomas, R. K.; Lu, J. R. Surface composition of mixed surfactant monolayers at concentrations well in excess of the cmc, a neutron scattering study, *Langmuir*, **1993**, 9, 1651-1656

TABLE OF CONTENT GRAPHIC

Mixing natural and synthetic surfactants: co-adsorption of triterpenoid saponins and sodium dodecyl sulfate at the air-water interface.

I M Tucker, A Burley, R E Petkova, S L Hosking, J Penfold, R K Thomas, P X Li, J R P Webster, R Welbourn

